



New Hybrid Anion Exchanger for Fluoride Removal

Othman Hakami

Chemistry Department, Faculty of Science, Jazan University, Jazan, KSA, Saudi Arabia

Nat. Env. & Poll. Tech.
Website: www.neptjournal.com

Received: 06-04-2016

Accepted: 24-05-2016

Key Words:

Fluoride removal
A500P
Zr oxide
Resin

ABSTRACT

Contamination of groundwater by fluoride from both anthropogenic and natural sources is an issue of major concern. Anion exchanger A500P was loaded with Zr ions and precipitated with sodium hydroxide, followed by thermal treatment at 60°C, to form hydrated Zr oxide. Fluoride removal using Zr-loaded A500P from solutions with a fluoride concentration of 5 mgL⁻¹ was investigated and compared with that using activated alumina, by performing batch tests under different experimental conditions. The results indicated that fluoride adsorption occurs immediately over the entire surface of the A500P Zr-loaded resin, as well as over activated alumina (the equilibrium has been reached after 6 h). The obtained data indicated the relatively high removal activity of Zr-loaded A500P as compared to that of activated alumina. Furthermore, competitive species such as SO₄²⁻ and PO₄³⁻ strongly affected the rate of fluoride removal; at sulphate and phosphate doses of 1000 ppm and 1 ppm, respectively, fluoride removal was completely suppressed. Experiments performed over the pH range 2-10 indicated that the rate of fluoride removal is inversely proportional to pH; that is, a lower pH results in higher removal capacity.

INTRODUCTION

Fluoride present in drinking water has substantial benefits for human health, however, fluoride has also been reported to have numerous adverse impacts. Fluoride aids in the effective development of organs in human beings. Generally, low concentrations of fluoride are added to drinking water for preventing dental caries and strengthening teeth (WHO 2006, Ayoob & Gupta 2006). Maintaining the fluoride concentration to below the acceptable limit (1.5 mgL⁻¹) in the diet can help minimize damage to the teeth and bones (Solangi et al. 2009). However, higher fluoride concentrations can result in dental and skeletal fluorosis, in addition to injury to the endocrine glands, liver, and thyroid etc. (Daifullah et al. 2007, Ghosh et al. 2013, Roy & Dass 2013). Researchers across the globe, i.e. from India, China, Africa, Pakistan, etc., have undertaken significant efforts to identify and mitigate the adverse health effects of fluoride (Wang et al. 2007, Agrawal 2013, Yasmin et al. 2013, Lutz et al. 2013, Kravchenko et al. 2014, Solangi et al. 2009).

Several methods are used for the removal of excessive fluoride from drinking water, such as adsorption (Asgari et al. 2012, Chatterjee & De 2014), ion exchange (Meenakshi & Viswanathan 2007, Viswanathan & Meenakshi 2009, Gong et al. 2012, Samadi et al. 2013), precipitation (Chen et al. 2012), and reverse osmosis, and filtration (Richards et al. 2010, Malaisamy et al. 2011, Chakraborty et al. 2013, Trikha & Sharma 2014).

Solid-phase extraction (SPE) is reported to be more efficient than other techniques such as liquid-liquid extraction

(Komjarova & Blust 2006, Vidal et al. 2012) for fluoride removal. Chelating resins are used in SPE to improve the extraction efficiency because of their stability and high ion sorption ability (Sharma & Pant 2009, Solangi et al. 2009). Iminodiacetate resins such as Chelex 100 and Amberlite IRC-718 are widely used as chelating resins for SPE (Agrawal et al. 2003, Yu et al. 2009), but they show poor selectivity (Rakhunde et al. 2012, Nasr et al. 2014). Other chelating resins employed for the aforementioned purpose are 4-vinyl pyridine-divinylbenzene/acrylonitrile-divinyl benzene copolymers (Metilda et al. 2005), Amberlite IRA-400 (Bayazit et al. 2011), silica-based C18 supports (Pesek et al. 2013), Amberlite A-26 (Dinarès et al. 2009), and modified poly (styrene-divinylbenzene) resin (Niu et al. 2010). Among Amberlite resins, Amberlite-XAD resins have excellent physicochemical properties that make them stable and durable in harsh environmental conditions (Ghasemi & Zolfonoun 2010, Xiao et al. 2012). Furthermore, Biswas and co-workers used synthetic iron(III)-aluminium(III) mixed oxide (Biswas et al. 2007), hydrous iron(III)-tin(IV) bimetal mixed oxide (Biswas et al. 2009), and synthetic iron(III)-aluminium(III)-chromium(III) ternary mixed oxide (Biswas et al. 2010) for the adsorption of fluoride. Chitosan beads (Bansiwal et al. 2009, Viswanathan et al. 2009) and magnetic chitosan particles (Ma et al. 2007) were also effectively used for the removal of fluoride by adsorption from aqueous solution. Maliyekkal et al. (2010) and Chen et al. (2011) designed and used a fixed bed column for the removal of fluoride from water. Recently, zirconium-modified nanoparticles (Zhang et al. 2012, Poursaberi et al. 2012),

gold nanoparticles (Xue et al. 2012), iron oxide nanoparticles (Raul et al. 2012), and magnetite nanoparticles (Chang et al. 2011) were used for fluoride removal.

In the current study, the filtering properties of Zr oxide have been modified by coating it on A500P resin. The modified Zr material was employed for fluoride removal from drinking water in batch tests and column runs, and the removal efficiency was compared with that observed when using activated alumina. The fluoride removal performance was evaluated as a function of the initial fluoride concentration in water and the amount of modified material used as the adsorbent.

MATERIALS AND METHODS

All chemical reagents used in this study were of analytical grade (AR). Activated alumina, sodium hydroxide, zirconium oxychloride, and sodium fluoride were purchased from Fisher Scientific, UK.

To prepare the adsorbent, 20 g of A500P was treated with 8% zirconium oxychloride, and the mixture was shaken for 24 h at room temperature. The obtained material was washed and treated with 5% NaOH solution to precipitate Zr as its hydroxide and then dried at 60°C overnight.

The adsorbent was characterized by X-ray Diffraction (XRD, Bruker, D8 Advance diffractometer, Billerica, USA) and Scanning Electron Microscopy (SEM, JEOL JSM-6360A).

Fluoride, phosphate, and sulphate measurements were performed by ion chromatography (Dionex Ion Pac®, UK) using an SRC18 column. The mobile phase comprised sodium carbonate and sodium bicarbonate (2:7 ratio), at a flow rate of 1.2 mL min⁻¹. In order to ensure a constant concentration of dissolved O₂, air was bubbled continuously into the reaction mixture.

All batch equilibrium experiments were carried out by mixing 200 mL of F⁻ solution at natural pH and other different pH levels, as well as at different doses of Zr-loaded A500p, activated alumina, sulphate and phosphate. The equilibrium concentrations were determined using Inductively Coupled Plasma (ICP), after filtration.

The amount of adsorbate F⁻ per gram of adsorbent (Q_{ads}, mol/g) and the maximum number of adsorbed molecules, Q_{max}, were determined according to the derived Langmuir equation after linearization:

$$Q_{\text{ads}} = \frac{Q_{\text{max}} K_{\text{ads}} C_{\text{eq}}}{1 + K_{\text{ads}} C_{\text{eq}}} \quad \dots(1)$$

The Freundlich parameters *K* and *n* were calculated using the classical formula, the results obtained for all the

concentrations studied ($C_{\text{eq}} = K C_0^n$).

Fixed bed column runs were carried out using a glass column (11 mm in diameter), constant-flow stainless steel pumps, and an ISCO fraction collector. Exhausted A500P loaded with Zr was regenerated using 0.5% NaOH.

RESULTS AND DISCUSSION

Characterization of Zr-loaded A500P

The X-ray diffractogram of the ion exchange (A500P) sample modified with Zr oxide is presented in Fig. 1b, in comparison with that of the parent A500P in Fig. 1a.

The hybrid ion exchange (HIX) samples have an amorphous structure because there are no diffraction peaks at

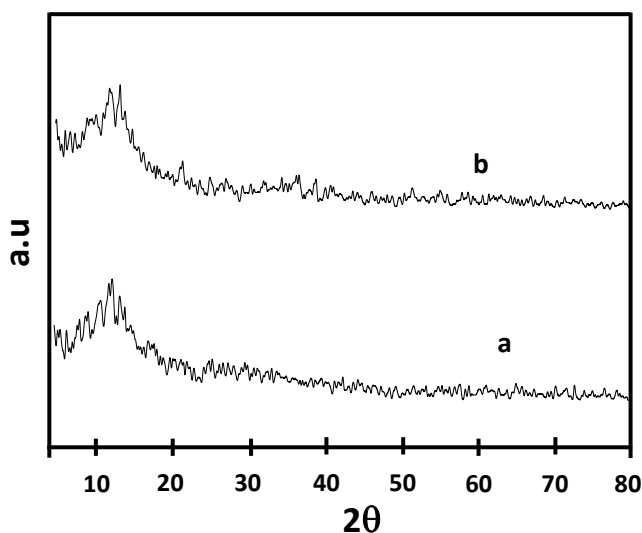


Fig. 1: XRD patterns of HIX modified by different cations: a) A500P b) Zr-A500P.

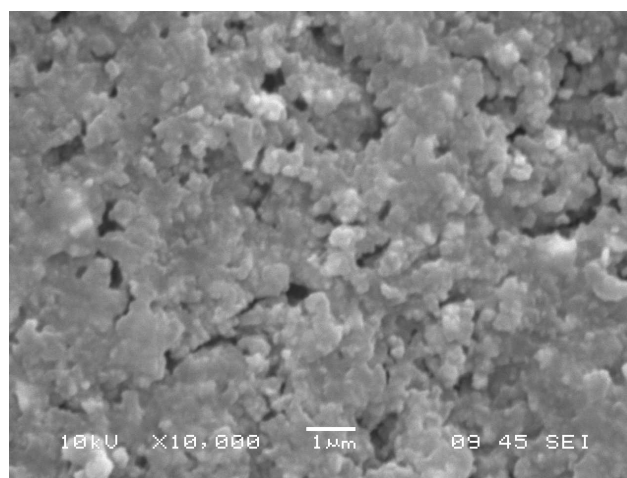


Fig. 2: SEM image of Zr-modified polymeric material (A500P).

tributable to Zr oxide or any crystalline species. It might be due to the small size of Zr oxide particles in the nano range (less than the detection limit of XRD).

The SEM image of the modified A500P ion exchange particles is shown in Fig. 2, and it can be seen that the particles appear to aggregate, which is due to the absence of any stabilizer in the reaction system during the preparation of Zr-modified A500P.

Fig. 3 illustrates the TEM image of the Zr-modified A500P. The obtained data indicate the presence of hydrated Zr oxide dispersed in the polymeric matrix. The data also indicate that the incorporated Zr particles have small sizes, of the order of 5 nm.

Adsorption of Fluoride on Zr-loaded A500P

The removal efficiency of a pollutant from water depends on the initial concentration of the concerned pollutant and the amount of adsorbent. A series of experiments were conducted in batch tests to evaluate the adsorption of fluoride

on the Zr-A500P surface at four different concentrations of catalyst: 0.05, 0.1, 0.15, and 0.2 gL⁻¹.

In all these experiments, Langmuir-type equilibrium adsorption was observed.

According to the Langmuir model, the coverage θ varies as

$$\theta = \frac{Q_{ads}}{Q_{max}} = \frac{KC_{eq}}{1 + KC_{eq}} \quad \dots(2)$$

Where, Q_{ads} is the number of adsorbed molecules at adsorption equilibrium, Q_{max} is the maximal adsorbable quantity, K is the Langmuir adsorption constant for F⁻ on Zr-A500P and activated alumina, and C_{eq} the concentration of F⁻ at adsorption equilibrium (Fig. 4).

Equation (3) represents the linear transformation of Eq. (2):

$$\frac{1}{Q_{ads}} = \frac{1}{Q_{max}} + \frac{1}{Q_{max} KC_{eq}} \quad \dots(3)$$

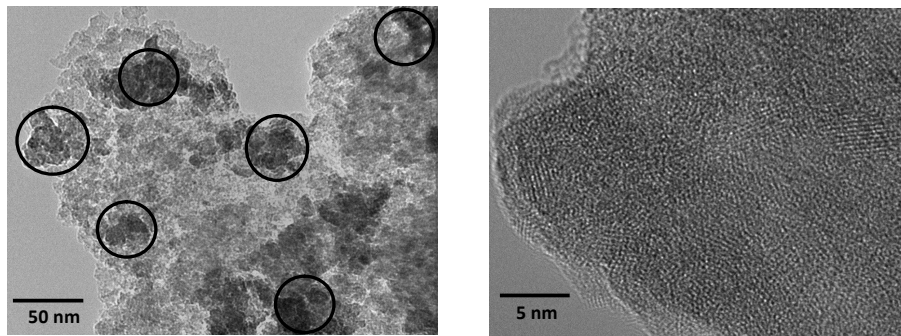


Fig. 3: TEM images of Zr-modified polymeric material (A500P).

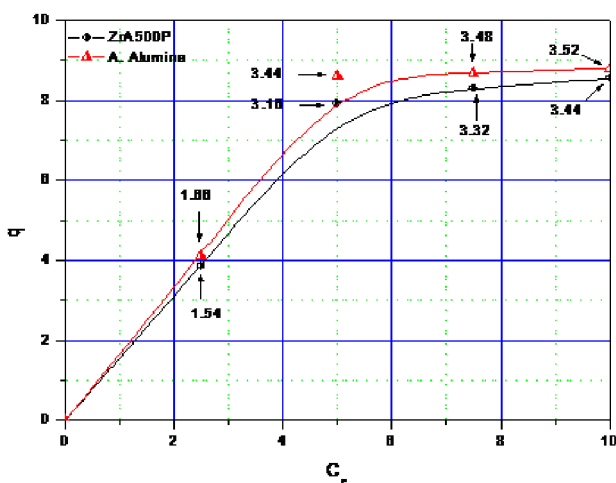


Fig. 4: Langmuir model for F⁻ adsorption on Zr-A500P and activated alumina.

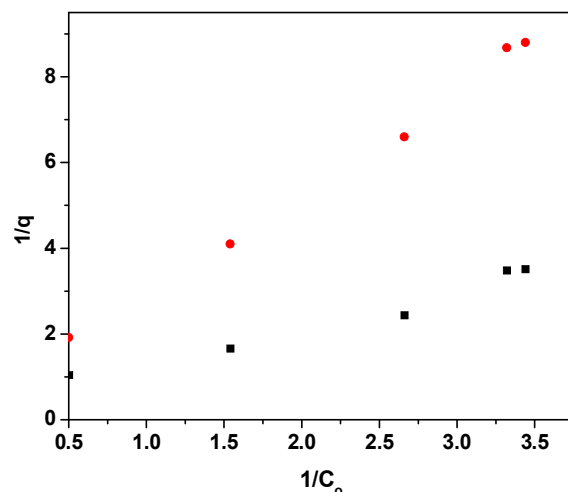


Fig. 5: Linear transformation Langmuir model for F⁻ adsorption on Zr-A500P and activated alumina.

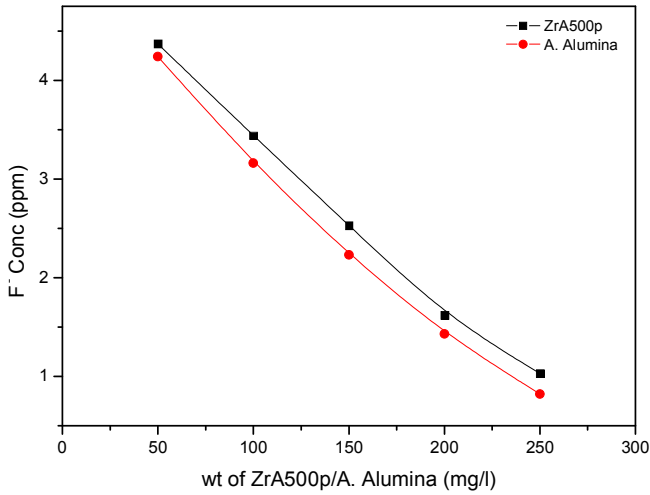


Fig. 6: Effect of adsorbent dose on F⁻ uptake.

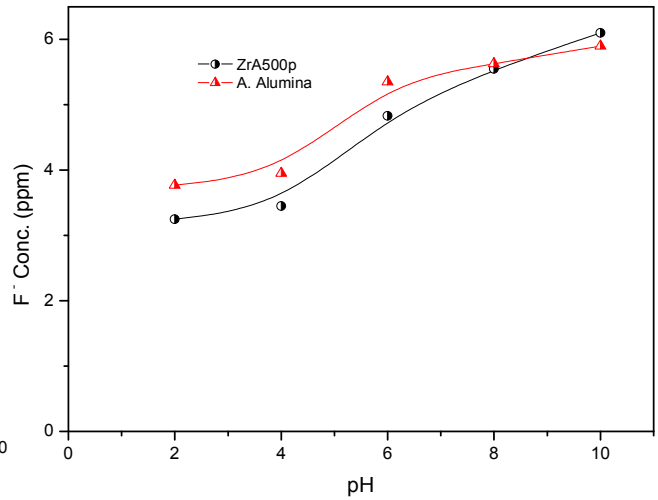


Fig. 7: Effect of pH on F⁻ uptake.

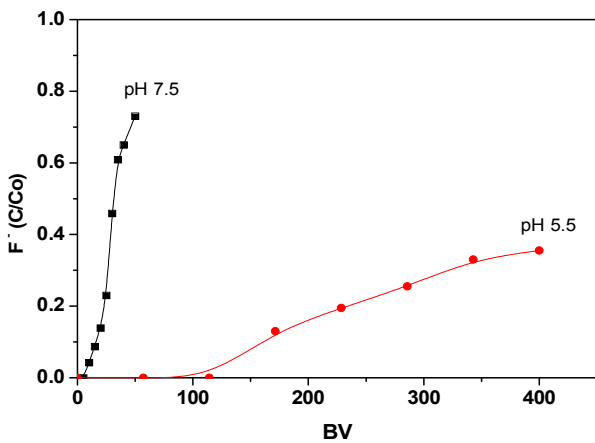


Fig. 8: Effluent history of column run for F⁻ removal over Zr-A500P at pH 5.5 and 7.5.

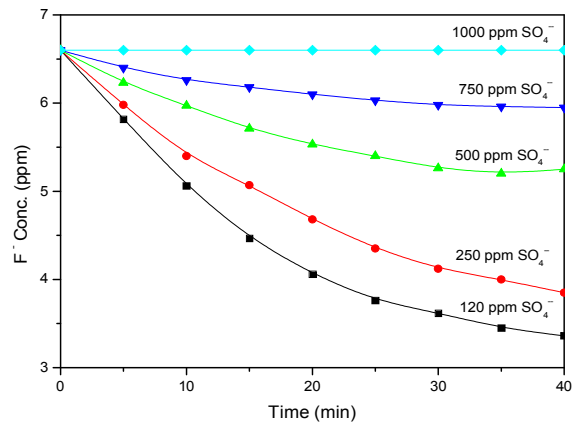


Fig. 9: Kinetics of sulfate effect on F⁻ removal.

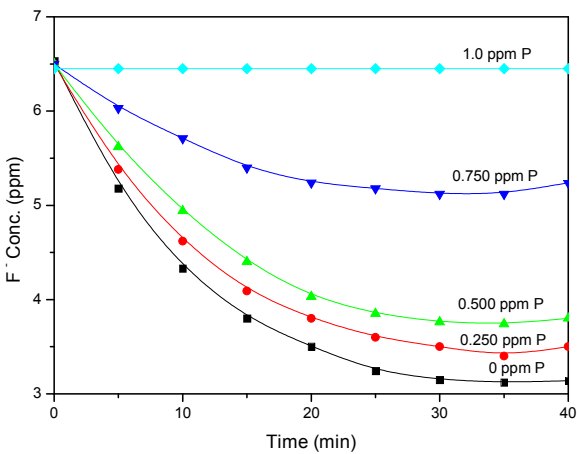


Fig. 10: Kinetics of phosphate effect on F⁻ removal.

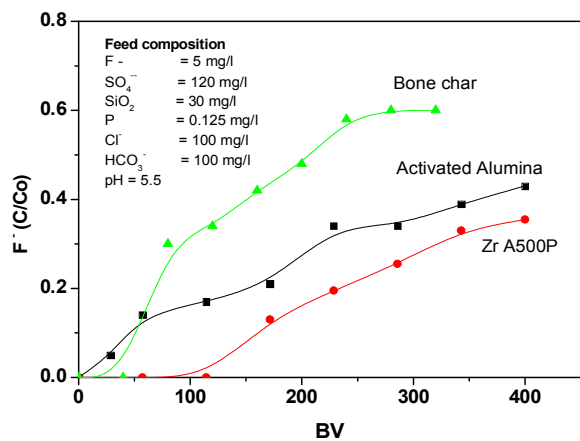


Fig. 11: Effluent history of column run for F⁻ removal over Zr-A500P, activated alumina and bone charcoal.

Therefore, a linear relation between $1/Q_{ads}$ and $1/C_e$ can be obtained with an intercept of $1/Q_{max}$ and a slope of $1/Q_{max}K$, where the values of Q_{max} and K can be calculated from the linear relation shown in Fig. 5. The data obtained indicate that $K = 0.54$ and $Q_{max} = 2.14 \text{ mg F. g}^{-1} \text{ resin}$.

Effect of Competing Anions on Fluoride Removal

Effect of adsorbent doses: The data obtained indicate the relative similarity between Zr-A500P and activated alumina upon variation of the adsorbent dose, as depicted in Fig. 6.

Effect of pH: Batch tests demonstrate that the amount of fluoride removed is dependent on pH. The results for Zr-A500P and activated alumina, with an initial F^- concentration of 6 mg/L over the pH range 2.0-10, are shown in Fig. 7. Good fluoride removal of 50% and 40% is observed at neutral pH for Zr-A500P and activated alumina, respectively. Furthermore, the data demonstrate that equilibrium fluoride concentration is directly proportional to pH; hence, it is possible to decrease the fluoride concentration to any level by selecting the appropriate $[H^+]/[F^-]$ ratio. The low rate of reaction at high pH could reflect the competition of OH^- with F^- for the surface adsorption sites.

The data obtained for the effect of pH during the column run indicate that 5.5 is the most efficient for fluoride removal. Fig. 8 shows that at pH 5.5, F^- breakthrough occurs for a bed volume of 300, whereas at pH 7.5, breakthrough occurs immediately at the start of the column run.

Effect of sulphate and phosphate: Competition between SO_4^{2-} (120-1000 mgL^{-1}) and PO_4^{3-} (0-1 mgL^{-1}) was investigated in batch tests; the obtained data are illustrated in Figs. 9 & 10. The data indicate that at low concentrations of SO_4^{2-} and PO_4^{3-} , the rates of F^- removal are very high. Furthermore, upon increasing the concentration of both SO_4^{2-} and PO_4^{3-} , the removal rate decreases and is completely suppressed at $1000 \text{ mgL}^{-1} SO_4^{2-}$ and $1 \text{ mgL}^{-1} PO_4^{3-}$.

Column Run

Under the optimum conditions for F^- removal, column runs were carried out with Zr-A500P and activated alumina in comparison with those for charcoal, which is one of the earliest adsorbents used for F^- removal. The data depicted in Fig. 11 show the effluent history of the column run for the removal of F^- . It is clear that F^- breakthrough starts after about 100 bed volumes for the Zr-A500P cycle, whereas breakthrough occurs immediately at the start of the column run for both activated alumina and charcoal.

CONCLUSIONS

Selectivity for fluoride removal was achieved by the modification of anion exchanger A500P with hydrated zirconium oxide.

The obtained data indicated the amorphous nature of the synthesized materials as well as the good dispersion of hydrated zirconium oxide on the surface of and inside the polymeric matrix. Furthermore, selectivity towards fluoride removal with the modified anion exchanger was better than that with activated alumina, in the batch tests and column runs.

ACKNOWLEDGMENT

This work was supported by Centre for the Environmental Research and Studies at Jazan University (CERS 3/2013).

REFERENCES

- Agrawal, A., Sahu, K. and Rawat, J. 2003. Kinetic studies on the exchange of bivalent metal ions on amberlite IRC 718-Animinodiacetate resin. *Solvent Extraction and Ion Exchange*, 21: 763-782.
- Agrawal, V. 2013. Groundwater contamination with fluoride in India: Sources, effects and prevention. *J. Dev. Manage.*, 1: 194.
- Asgari, G., Roshani, B. and Ghanizadeh, G. 2012. The investigation of kinetic and isotherm of fluoride adsorption onto functionalize pumice stone. *J. Hazard. Mater.*, 217: 123-132.
- Ayoob, S. and Gupta, A. 2006. Fluoride in drinking water: A review on the status and stress effects. *Crit. Rev. Env. Sci. Technol.*, 36: 433-487.
- Bansiwal, A., Thakre, D., Labhshetwar, N. Meshram, S. and Rayalu, S. 2009. Fluoride removal using lanthanum incorporated chitosan beads. *Colloids Surf., B: Biointerfaces*, 74: 216-224.
- Bayazit, S.A.S., Inci, I. S. and Uslu, H. 2011. Adsorption of lactic acid from model fermentation broth onto activated carbon and Amberlite IRA-67. *J. Chem. Eng. Data*, 56: 1751-1754.
- Biswas, K., Gupta, K. and Ghosh, U.C. 2009. Adsorption of fluoride by hydrous iron(III) - tin(IV) bimetal mixed oxide from the aqueous solutions. *Chem. Eng. J.*, 149: 196-206.
- Biswas, K., Gupta, K., Goswami, A. and Ghosh, U.C. 2010. Fluoride removal efficiency from aqueous solution by synthetic iron(III)-aluminum(III)-chromium(III) ternary mixed oxide. *Desalination*, 255: 44-51.
- Biswas, K., Saha, S.K. and Ghosh, U.C. 2007. Adsorption of fluoride from aqueous solution by a synthetic iron(III)-aluminum(III) mixed oxide. *Ind. Eng. Chem. Res.*, 46: 5346-5356.
- Chakraborty, S., Roy, M. and Pal, P. 2013. Removal of fluoride from contaminated groundwater by cross flow nano filtration: Transport modeling and economic evaluation. *Desalination*, 313: 115-124.
- Chang, Q., Zhu, L., Luo, Z., Lei, M., Zhang, S. and Tang, H. 2011. Sono-assisted preparation of magnetic magnesium-aluminum layered double hydroxides and their application for removing fluoride. *Ultrason. Sonochem.*, 18: 553-561.
- Chatterjee, S. and De, S. 2014. Adsorptive removal of fluoride by activated alumina doped cellulose acetate phthalate (CAP) mixed matrix membrane. *Sep. Purif. Technol.*, 125: 223-238.
- Chen, L., He, B.Y., He, S., Wang, T.J., Su, C.L. and Jin, Y. 2012. Fe-Ti oxide nano-adsorbent synthesized by co-precipitation for fluoride removal from drinking water and its adsorption mechanism. *Powder Technol.*, 227: 3-8.
- Chen, N., Zhang, Z., Feng, C., Li, M., Chen, R. and Sugiura, N. 2011. Investigations on the batch and fixed-bed column performance of fluoride adsorption by Kanuma mud. *Desalination*, 268: 76-82.

- Daifullah, A., Yakout, S. and Elreefy, S. 2007. Adsorption of fluoride in aqueous solutions using KMnO_4 modified activated carbon derived from steam pyrolysis of rice straw. *J. Hazard. Mater.*, 147: 633-643.
- Dinarès, I., de Miguel, C.G., Ibáñez, A., Mesquida, N. and Alcalde, E., 2009. Imidazolium ionic liquids: A simple anion exchange protocol. *Green Chemistry*, 11(10):1507-1510.
- Ghasemi, J.B. and Zolfonoun, E. 2010. Simultaneous spectrophotometric determination of trace amounts of uranium, thorium, and zirconium using the partial least squares method after their preconcentration by α -benzoin oxime modified Amberlite XAD-2000 resin. *Talanta*, 80: 1191-1197.
- Ghosh, A., Mukherjee, K., Ghosh, S.K. and Saha, B. 2013. Sources and toxicity of fluoride in the environment. *Res. Chem. Intermed.*, 39: 2881-2915.
- Gong, W.X., U, J.H., Liu, R.P. and Lan, H.C. 2012. Adsorption of fluoride onto different types of aluminas. *Chem. Eng. J.*, 189: 126-133.
- Komjarova, I. and Blust, R. 2006. Comparison of liquid-liquid extraction, solid-phase extraction and co-precipitation preconcentration methods for the determination of cadmium, copper, nickel, lead and zinc in seawater. *Anal. Chim. Acta.*, 576: 221-228.
- Kravchenko, J., Rango, T., Akushevich, I., Atlaw, B., Mccornick, P. G., Merola, R., Paul, C., Weinthal, E., Harrison, C. and Vengosh, A. 2014. The effect of non-fluoride factors on risk of dental fluorosis: Evidence from rural populations of the main Ethiopian rift. *Sci. Total Environ.*, 488: 595-606.
- Lutz, A., Diarra, S., Apambire, W.B., Thomas, J.M. and Ayamsegna, J. 2013. Drinking water from hand-pumps in Mali, Niger, and Ghana, West Africa: Review of health effects. *J. Water Resource Prot.*, 5: 13.
- Ma, W., Ya, F.Q., Han, M. and Wang, R. 2007. Characteristics of equilibrium, kinetics studies for adsorption of fluoride on magnetic-chitosan particle. *J. Hazard. Mat.*, 143: 296-302.
- Malaisamy, R., Talla-Nwafo, A. and Jones, K.L. 2011. Polyelectrolyte modification of nanofiltration membrane for selective removal of monovalent anions. *Sep. Purif. Technol.*, 77: 367-374.
- Maliyekkal, S.M., Antony, K. and Pradeep, T. 2010. High yield combustion synthesis of nanomagnesia and its application for fluoride removal. *Sci. Total Environ.*, 408: 2273-2282.
- Meenakshi, S. and Viswanathan, N. 2007. Identification of selective ion-exchange resin for fluoride sorption. *J. Colloid Interface Sci.*, 308: 438-450.
- Metilda, P., Sanghamitra, K., Mary Gladis, J., Naidu, G. and Prasada Rao, T. 2005. Amberlite XAD-4 functionalized with succinic acid for the solid phase extractive preconcentration and separation of uranium (VI). *Talanta*, 65: 192-200.
- Nasr, A.B., Charcosset, C., Amar, R.B. and Walha, K. 2014. Fluoride removal from aqueous solution by Purolite A520E resin: kinetic and thermodynamics study. *Desalin. Water Treat.*, 1-8.
- Niu, L., Deng, S., Yu, G. and Huang, J. 2010. Efficient removal of Cu(II), Pb(II), Cr(VI) and As(V) from aqueous solution using an aminated resin prepared by surface-initiated atom transfer radical polymerization. *Chem. Eng. J.*, 165: 751-757.
- WHO 2006. Guidelines for Drinking-Water Quality: First Addendum to Volume 1, Recommendations, World Health Organization.
- Pesek, J.J., Matyska, M.T., Boysen, R.I., Yang, Y. and Hearn, M.T. 2013. Aqueous normal-phase chromatography using silica-hydride-based stationary phases. *TrAC Trend. Anal. Chem.*, 42: 64-73.
- Poursaberi, T., Hassanisadi, M., Torkestani, K. and Zare, M. 2012. Development of zirconium (IV)-metalloporphyrin grafted Fe_3O_4 nanoparticles for efficient fluoride removal. *Chem. Eng. J.*, 189: 117-125.
- Rakhunde, R., Deshpande, L. and Juneja, H. 2012. Chemical speciation of chromium in water: a review. *Crit. Rev. Env. Sci. Technol.*, 42: 776-810.
- Raul, P.K., Devi, R.R., Umlong, I.M., Banerjee, S., Singh, L. and Purkait, M. 2012. Removal of fluoride from water using iron oxide-hydroxide nanoparticles. *J. Nanosci. Nanotechnol.*, 12: 3922-3930.
- Richards, L.A., Vuachere, M. and Schäfer, A.I. 2010. Impact of pH on the removal of fluoride, nitrate and boron by nanofiltration/reverse osmosis. *Desalination*, 261: 331-337.
- Roy, S. and Dass, G. 2013. Fluoride contamination in drinking water-a review. *J. Resour. Environ.*, 3: 53-58.
- Samadi, M.T., Sepehr, M.N., Zarrabi, M., Ramhormozi, S.M., Azizan, S. and Amrane, A. 2013. Removal of fluoride ions by ion exchange resin: Kinetic and equilibrium studies. *Environmental Engineering and Management Journal*, 13(1): 205-214.
- Sharma, R. and Pant, P. 2009. Preconcentration and determination of trace metal ions from aqueous samples by newly developed gallic acid modified Amberlite XAD-16 chelating resin. *J. Hazard. Mater.*, 163: 295-301.
- Solangi, I.B., Memon, S. and Bhangar, M. 2009. Removal of fluoride from aqueous environment by modified Amberlite resin. *J. Hazard. Mater.*, 171: 815-819.
- Trikha, R. and Sharma, B.K. 2014. Studies on factors affecting fluoride removal from water using passive system. *J. Environ. Chem. Eng.*, 2: 172-176.
- Vidal, L., Reikkola, M.L. and Canals, A. 2012. Ionic liquid-modified materials for solid-phase extraction and separation: a review. *Anal. Chim. Acta*, 715: 19-41.
- Viswanathan, N. and Meenakshi, S. 2009. Role of metal ion incorporation in ion exchange resin on the selectivity of fluoride. *J. Hazard. Mat.*, 162: 920-930.
- Viswanathan, N., Sundaram, C.S. and Meenakshi, S. 2009. Removal of fluoride from aqueous solution using protonated chitosan beads. *J. Hazard. Mater.*, 161, 423-430.
- Wang, S.X., Wang, Z.H., Cheng, X.T., Li, J., Sang, Z.P., Zhang, X.D., Han, L.L., Qiao, X.Y., Wu, Z.M. and Wang, Z.Q. 2007. Arsenic and fluoride exposure in drinking water: Children's IQ and growth in Shanyin county, Shanxi province, China. *Environ. Health Perspect.*, 115: 643.
- Xiao, F., Davidsavor, K.J., Park, S., Nakayama, M. and Phillips, B.R. 2012. Batch and column study: Sorption of perfluorinated surfactants from water and cosolvent systems by Amberlite XAD resins. *J. Colloid Interface Sci.*, 368: 505-511.
- Xue, M., Wang, X., Duan, L., Gao, W., Ji, L. and Tang, B. 2012. A new nanoprobe based on FRET between functional quantum dots and gold nanoparticles for fluoride anion and its applications for biological imaging. *Biosens. Bioelectron.*, 36: 168-173.
- Yasmin, S., Ranjan, S., Hilaluddin, D'souza, D. 2013. Effect of excess fluoride ingestion on human thyroid function in Gaya region, Bihar, India. *Toxicol. Environ. Chem.*, 95: 1235-1243.
- Yu, Z., Qi, T., Qu, J., Wang, L. and Chu, J. 2009. Removal of Ca (II) and Mg (II) from potassium chromate solution on Amberlite IRC 748 synthetic resin by ion exchange. *J. Hazard. Mater.*, 167: 406-412.
- Zhang, G., He, Z. and Xu, W. 2012. A low-cost and high efficient zirconium-modified-Na-attapulgite adsorbent for fluoride removal from aqueous solutions. *Chem. Eng. J.*, 183: 315-324.